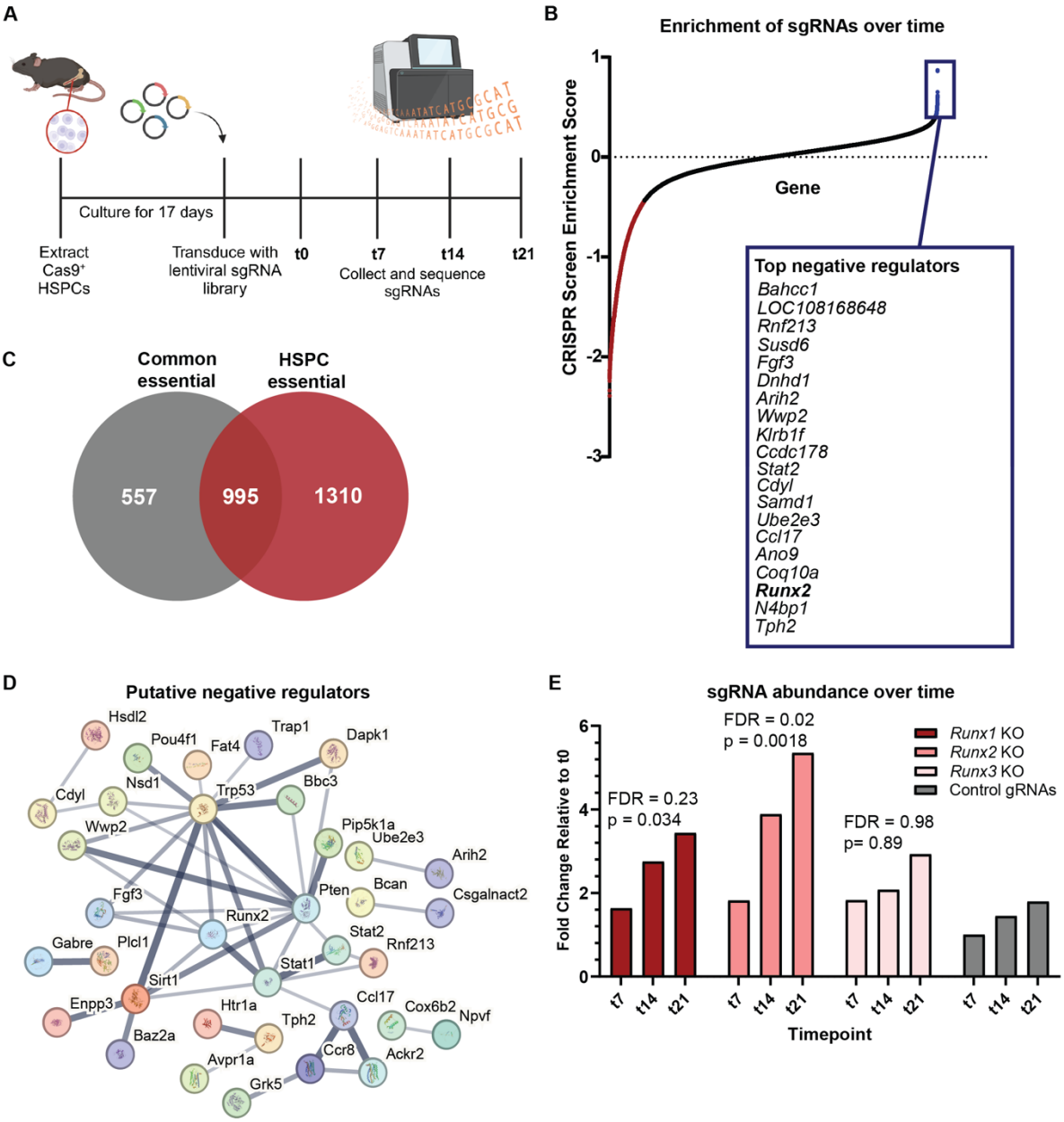
Figures and legends

Figure 1: Genome-wide ex vivo HSPC CRISPR screen identifies putative regulators of expansion



(A) Schematic overview of *ex vivo* HSPC CRISPR KO screen for top putative negative regulators. Created in BioRender.

(B) Beta-score for the 21,601 genes targeted in the *ex vivo* HSPC expansion screen. Inset: Top 20 beta-score genes listed within insert.

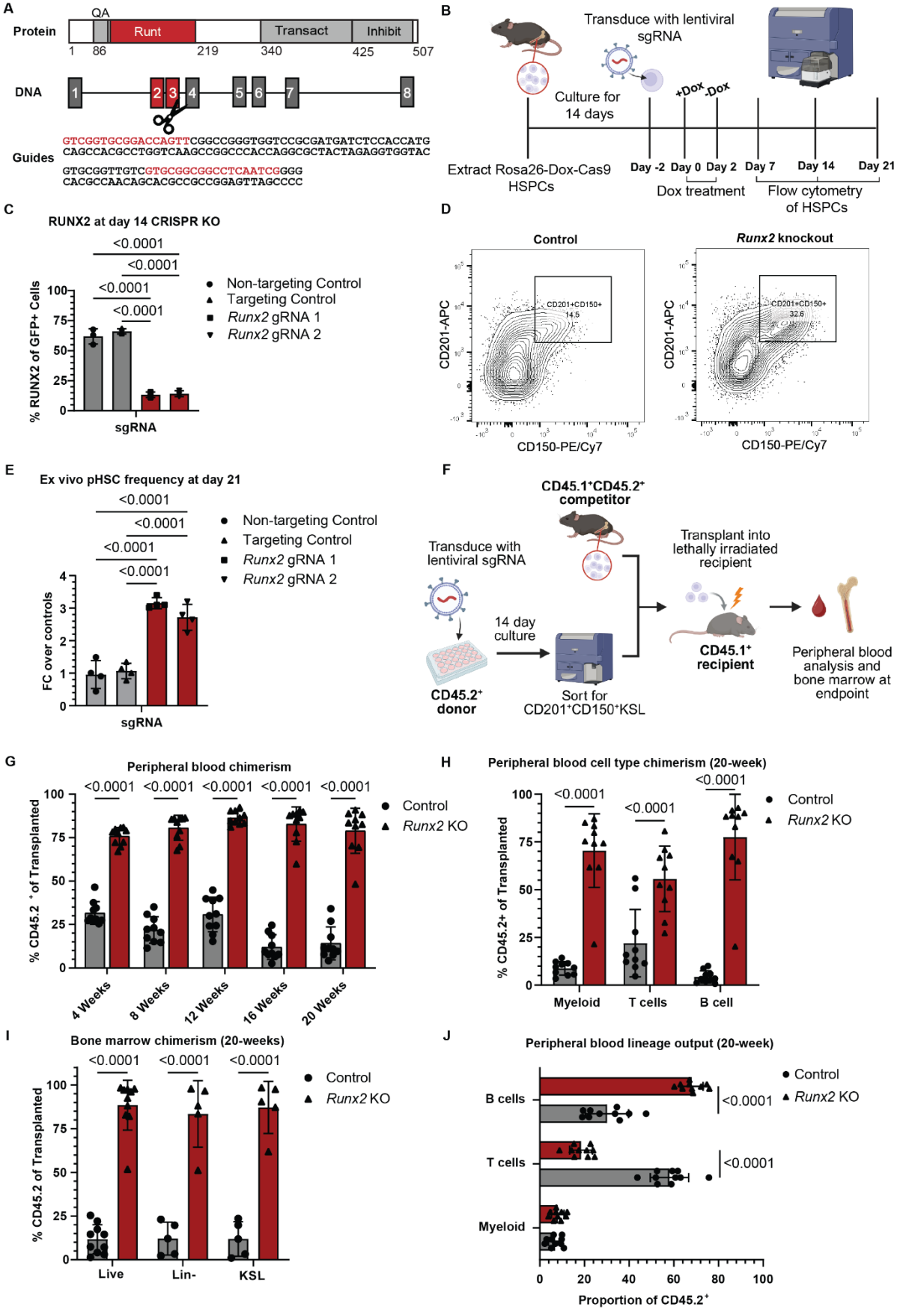
(C) Venn diagram of the overlap in essential genes from Achilles common essential list[31] and the essential genes identified in our HSPC screen.

(D) STRING analysis of protein-protein interactions of genes with positive beta value and FDR < 10%. Thicker line = stronger reported interaction. Interactions can be: from curated

databases, experimentally determined, gene neighbourhood, gene fusions, gene co-occurrence, textmining, co-expression and protein homology.

(E) Time course of sgRNA-expressing cells over time for the three *Runx* genes and control gRNAs, normalised to t0. FDR and p-values from the screen analysis shown above.

Figure 2: CRISPR-mediated KO of Runx2 enhances HSC expansion and engraftment



(A) Schematic of *Runx2*-targeting sgRNAs.

(B) Schematic overview of the experiment. Two guides targeting *Runx2* and two control guides (one non-targeting and one targeting the safe harbour locus *Rosa26*) were used. Created in BioRender.

(C) Intracellular flow cytometric analysis for RUNX2 in control and *Runx2*-KO HSPC cultures. n = 3.

(D) Representative flow cytometry plots showing differences in pHSC ($CD201^{+}CD150^{+}cKit^{+}Sca1^{+}Lineage^{-}$) populations *ex vivo* in *Runx2*-KO and control HSPC cultures.

(E) *Ex vivo* pHSC frequency at 21 days. See **Figure S2C** for data for days 0-14. Data normalised to controls. n = 4.

(F) Experimental overview of competitive transplant assay following *ex vivo* culture of $cKit^{+}$ cells from C57BL/6-Gt(ROSA)26Sor$^{tm1(rtTA*M2)Jae}$ Col1a1$^{tm1(tetO-cas9)Sho}$ doxycycline-inducible Cas9 mice. 2000 donor $CD45.2^{+}$ pHSCs alongside 1 million $CD45.1^{+}CD45.2^{+}$ whole bone marrow cells were transplanted into lethally irradiated $CD45.1^{+}$ recipient mice. Created in BioRender.

(G) Peripheral blood donor chimerism over 20 weeks following transplantation. n = 10. 2-way ANOVA was performed.

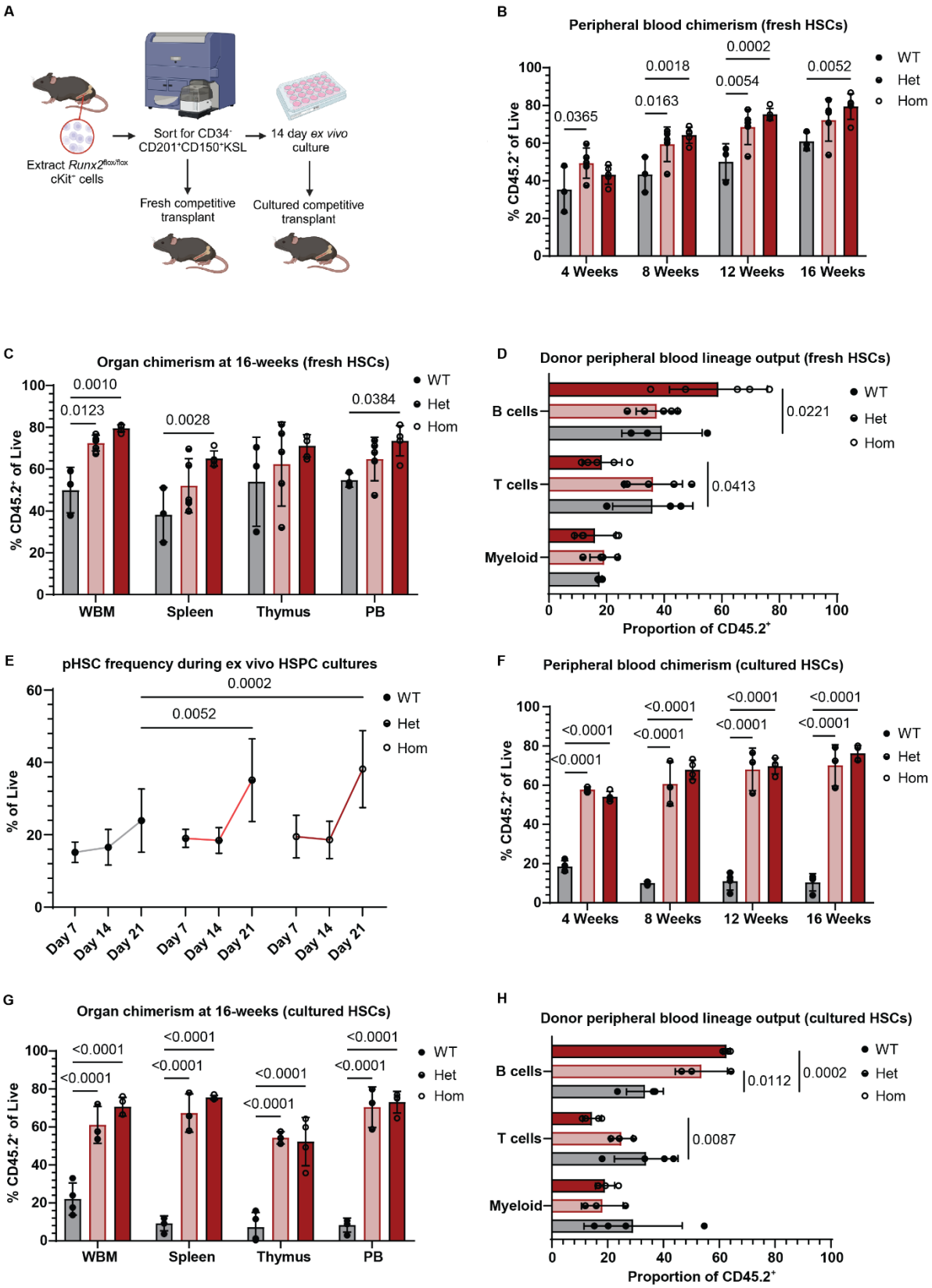
(H) Donor chimerism within peripheral blood myeloid, T and B cell compartments at the 20-week endpoint. 2-way ANOVA was performed.

(I) Bone marrow donor chimerism at the 20-week transplant endpoint. n = 10. 2-way ANOVA was performed.

(J) Proportion of myeloid, B and T cells within the $CD45.2^{+}$ donor peripheral blood cell compartment at the 20-week endpoint. n = 10. 2-way ANOVA was performed.

Non-significance not labelled.

Figure 3: Heterozygous loss of Runx2 is sufficient to drive increased HSC expansion and reconstitution potentials



(A) Experimental overview for assays exploring the phenotypes of homozygous and heterozygous *Runx2* KO HSCs. Created in BioRender.

(B) Peripheral blood chimerism from transplantation assays using 100 fresh $CD45.2^+$ HSCs vs 0.5 million $CD45.1^+CD45.2^+$ WBM competitor cells. n = 3-5. 2-way ANOVA was performed.

(C) Donor chimerism within whole bone marrow (WBM), spleen, thymus and peripheral blood (PB) chimerism of competitive transplant assay using 100 fresh $CD45.2^+$ HSCs. n = 3-5. 2-way ANOVA was performed.

(D) 16-week peripheral blood lineage output of competitive transplant assay using 100 fresh sorted $CD45.2^+$ HSCs. n = 3-5. 2-way ANOVA was performed.

(E) *Ex vivo* pHSC frequency over three-week culture. n = 6.

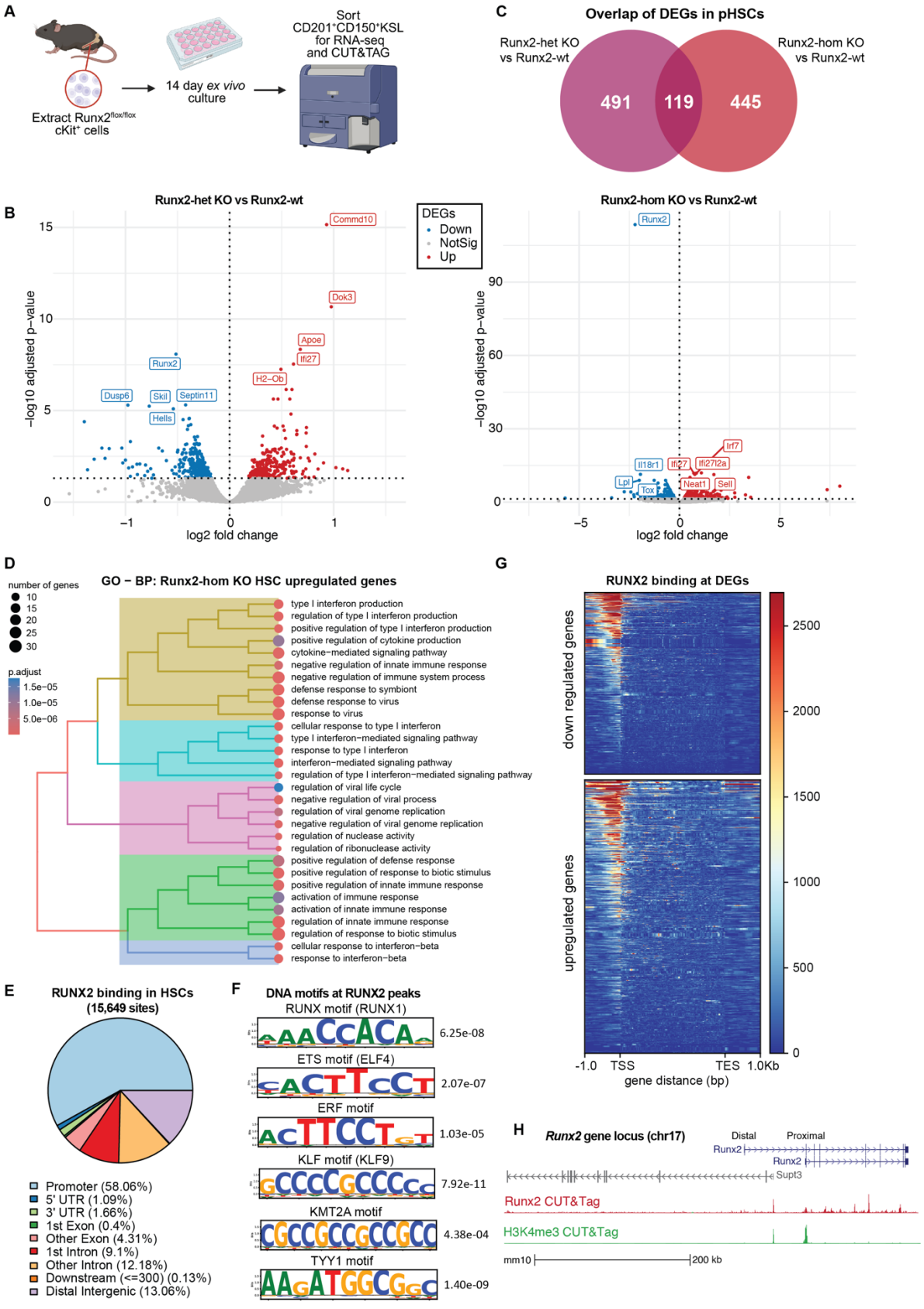
(F) Peripheral blood chimerism from transplantation assays using 10,000 $CD45.2^+$ cultured HSPCs vs 1 million $CD45.1^+CD45.2^+$ WBM competitor cells. n = 3-4. 2-way ANOVA was performed.

(G) Donor chimerism within WBM, spleen, thymus and PB from transplantation assays using 10,000 $CD45.2^+$ 14-day cultured HSPCs. n = 3-4. 2-way ANOVA was performed.

(H) 16-week peripheral blood lineage output of competitive transplant assay using 10,000 $CD45.2^+$ 14-day cultured HSPCs. n = 3-4. 2-way ANOVA was performed.

Non-significance not labelled.

Figure 4: Loss.of.Runx8.causes.context_specific.transcriptional.changes



(A) Experimental overview for RNA-seq and CUT&Tag on cultured pHSCs ($CD201^+CD150^+KSL$). Created in BioRender.

(B) Volcano plot of differentially expressed genes (DEGs) for *Runx2*-het KO vs *Runx2*-wt (left plot) and *Runx2*-hom KO vs *Runx2*-wt (right plot) in pHSCs.

(C) Gene overlap for *Runx2*-hom KO vs *Runx2*-wt DEGs and *Runx2*-het KO vs *Runx2*-wt DEGs in pHSCs (for DEGs with adjusted $p<0.05$).

(D) Top 30 upregulated Gene Ontology Biological Process for *Runx2*-hom KO vs *Runx2*-wt pHSC RNA-seq.

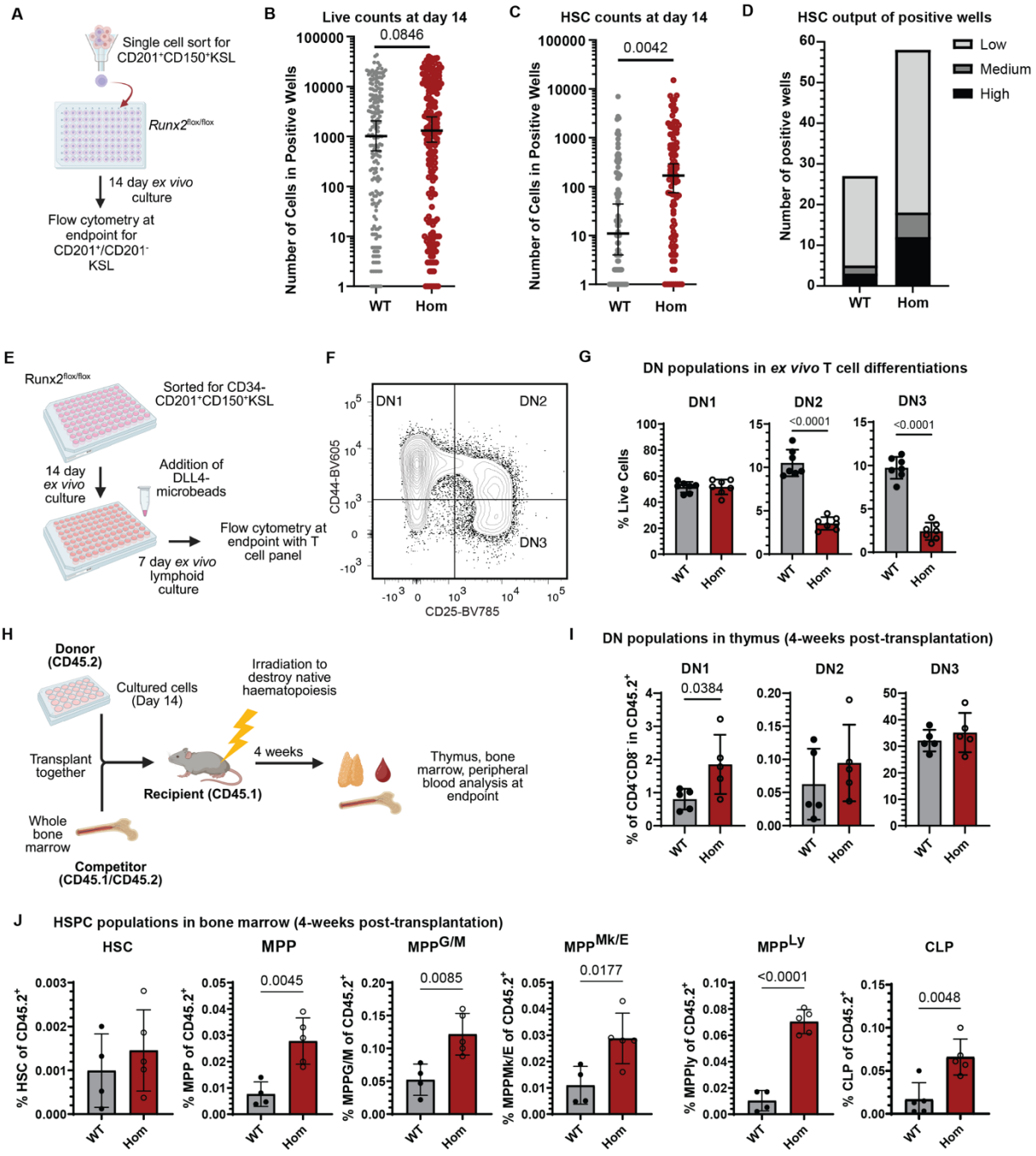
(E) Genomic features present at RUNX2 peaks in *Runx2-wt* pHSCs.

(F) Top 6 motifs present in RUNX2-bound promoters after filtered by genes expressed in *Runx2*-wt pHSC RNA-seq. p-value calculated using a null model consisting of sampling motif columns from all the columns in the set of target motifs.

(G) RUNX2 binding across promoters in DEGs from *Runx2*-hom KO vs *Runx2*-wt pHSC RNA-seq.

(H) Genome track of the *Runx2* gene locus showing RUNX2 and H3K4me3 CUT&Tag in *Runx2*-wt pHSCs.

Figure 5: Loss of Runx2 enhances HSC self-renewal but decreases T-cell commitment



(A) Experimental overview for *ex vivo* clonal plating assays of *Runx2*-hom KO HSCs. Created in BioRender.

(B) Number of live cells per positive well 14 days after single cell plating of CD201^{+}CD150^{+}KSL. n = 190. Line at median with 95% CI. Unpaired T-test was performed.

(C) Number of CD201^{+}KSL live cells in wells 14 days after single cell plating of CD201^{+}CD150^{+}KSL. n = 190. Line at median with 95% CI. Unpaired T-test was performed.

(D) Clonal identities at 14-days after single cell plating and percentage of wells with this identity. Low output clones = 5-50% $CD201^{+}KSL$, Medium output clones = 50-75% $CD201^{+}KSL$, High output clones = > 75% $CD201^{+}KSL$.

(E) Experimental overview for *ex vivo* T-cell differentiation assays of *Runx2*-hom HSCs. Created in BioRender.

(F) Representative flow plot of *ex vivo* T-cell differentiation generating DN1 to DN3 stages after 7-days.

(G) Frequency of DN1 to DN3 stage cells generated in *ex vivo* T-cell differentiation assays. n = 7, unpaired T-test was performed.

(H) Experimental overview for 4-week competitive transplantation assay. Created in BioRender.

(I) Frequency of DN1 to DN3 stage cells in $CD45.2^{+}$ donor derived $CD8^{-}CD8^{-}$ cells in the thymus of recipient mice at 4-week endpoint. n = 5, unpaired T-test was performed.

(J) Frequency of immunophenotypic HSPC populations in donor derived bone marrow of recipient mice at 4-week endpoint. n = 5, unpaired T-test was performed. HSC = $CD150^{+}CD48^{-}KSL$, MPP = $CD150^{-}CD48^{-}Flt3^{-}KSL$, $MPP^{G/M}$ = $CD150^{+}CD48^{-}Flt3^{-}KSL$, $MPP^{Mk/E}$ = $CD150^{+}CD48^{+}Flt3^{-}KSL$, MPP^{Ly} = $CD150^{-}Flt3^{+}KSL$, CLP = $CD127^{+}KSL$.

Non-significance not labelled.